



MAGIC-TDAS 05-10
050607 / MMeyer

Calibration of the MAGIC telescope using muon rings

M. Meyer (Lehrstuhl für Astronomie, Universität
Würzburg)

07 June 2005

Abstract

Muons hitting the reflector of the MAGIC telescope images a ring in the focal plane with radius equal to the Čerenkov angle.

As the geometry can be easily reconstructed, the muon events can be separated from other events.

For the analysis new image parameters are introduced. These are the radius of the ring (Radius), its width (ArcWidth), its opening angle (ArcPhi) and its total light content, measured in photo-electrons (Muon-Size). The agreement to muon events from Monte Carlo simulations is acceptable.

Comparing the relative ring broadening of muons, taken from observational data, with simulated muon data of different point-spread functions (psf) allows to calculate the psf of the reflector with an error of $\sim 15\%$.

By comparing the energy dependent total light content of muons from observational and simulated data the overall light efficiency can be calculated with an accuracy of $\sim 3\%$.

The analysis is now full implemented in the standard analysis chain. The psf as well as the light efficiency are available for all MAGIC data since june 2004 in the database.

The psf shows an evolution, starting from 11 mm after the new mirror alignment in july 2004 to nearly 17 mm after a bad weather period in february 2005.

The energy dependent light content is in good agreement to a 27% reduced simulation output. A difference of $\sim 3\%$ between data, where the signal is extracted by the DigitalFilter and those, where the Spline-method was used, could be found.

It was also possible to identify data samples, where the quality was bad or the calibration didn't work properly.

Contents

1	Introduction	3
2	Analytical description of muon images in IACTs	3
2.1	Muon image depending on impact parameter	3
2.2	Broadening of the muon ring image	5
3	Method	7
3.1	Calculation of the image parameters	7
3.2	Simulation	9
3.3	Results	9
3.4	Point-Spread function and overall light efficiency	9
4	Automatisation	11
4.1	Implementation in the standard analysis chain	11
4.2	Simplification of the psf and light collection efficiency calculation .	11
5	Stability and performance study	12
5.1	Muon rate	12
5.2	Point-spread function	13
5.3	Calibration	14
6	Summary	14
A	Overview	17
B	Point-spread function	18
C	Calibration	22

1 Introduction

Muons derived from hadronic showers reach the observation level of the MAGIC telescope. From [1] a integral flux of about $17.9 \text{ m}^{-2} \text{ s}^{-1} \text{ sr}^{-1}$ over 6 GeV is expected, which corresponds to a rate of $\sim 4 \text{ Hz}$ for muons, hitting the reflector with an inclination angle $\leq 1^\circ$. The measured rate is lower by a factor of three, because of different selection criteria and the possibility of coincidence with electro-magnetic subshowers.

Isolated muons give characteristic ring images in the camera. As the geometry can be easily reconstructed muons are a powerful tool for monitoring the behaviour of the telescope like the point-spread-function (psf) and the overall light efficiency [2].

In the following section, the properties of the muon images are described in an analytical way. The third section shows the method and refers to the used classes in the Magic analysis and reconstruction software (Mars) package. The fourth section contents instructions for analysers how to use the classes and how to work with automatic muon parameter calculation. The last section gives an overview over the results from the data since june 2004.

2 Analytical description of muon images in IACTs

When a muon hits the reflector, the Čerenkov light cone images a ring in the camera plane. Due to the inclination angle of the muon track, the ring image is shifted out of the center of the camera. If the muon track goes beside the mirror dish, only a fraction of the light cone can be seen, resulting in ring fraction (arc) in the camera plane.

2.1 Muon image depending on impact parameter

For an analytical description of the intensity distribution along the ring (azimuthal intensity distribution) it is better first to distinguish between muon impact inside and outside the mirror dish. The impact parameter p is defined as the distance from the center of the mirror to the impact point of the muon in the plane normal to the optical axis (fig.1). The amount of photons per path dh and azimuth angle $d\phi$, which are emitted from a single muon and reflected by the mirror is:

$$\frac{d^2N}{dh d\phi} = \alpha \int_{\lambda_1}^{\lambda_2} \frac{\psi(\lambda)}{\lambda^2} \left(1 - \frac{1}{\beta^2 n^2(\lambda)} \right) d\lambda \quad (1)$$

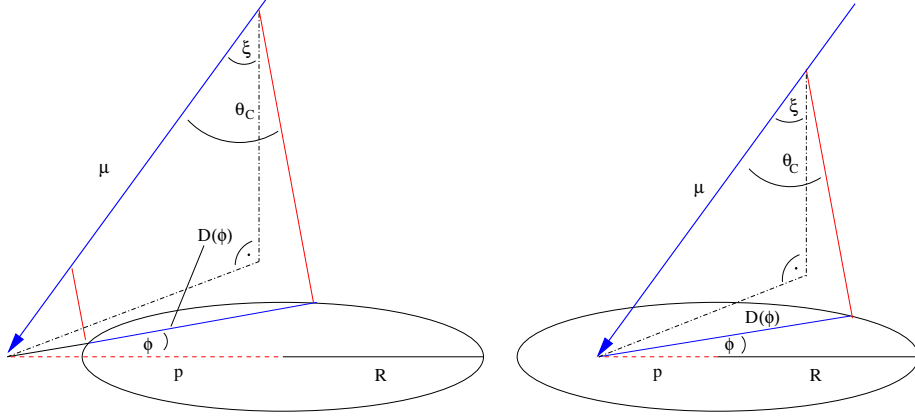


Figure 1: Muon impact outside (left) and inside the mirror dish (right). p = impact parameter; R = mirror radius; ξ = inclination angle; θ_C = Čerenkov angle.

with $\psi(\lambda)$ as the photon-collection-efficiency of the mirror. with $n(\lambda) \approx n$ and $1/\beta^2 n^2 = \cos \theta$ one gets:

$$\frac{d^2 N}{dh d\phi} = \alpha \sin^2 \theta \int_{\lambda_1}^{\lambda_2} \frac{\psi(\lambda)}{\lambda^2} d\lambda. \quad (2)$$

Definition: $I = \int_{\lambda_1}^{\lambda_2} \frac{\psi(\lambda)}{\lambda^2} d\lambda$

After inserting in equation 2 one gets in a second order approximation in ξ :

$$\begin{aligned} \frac{d^2 N}{dh d\phi} &= I \alpha \sin^2 \theta \\ \frac{dN}{d\phi} &= I \alpha \sin^2 \theta \frac{D(\phi)}{\tan \theta} = I \frac{\alpha}{2} \sin(2\theta) D(\phi) \end{aligned} \quad (3)$$

For muon impact $p > R$, one gets:

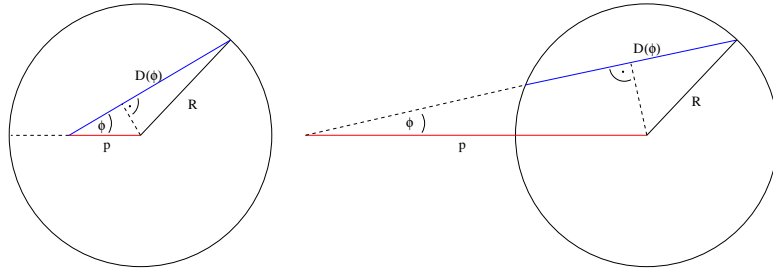


Figure 2: Muon impact inside (left) and outside the mirror (right)

$$D(\phi) = 2R\sqrt{1 - \left(\frac{p}{R}\right)^2 \sin^2 \phi} \quad (4)$$

For $p \leq R$ one gets:

$$D(\phi) = R \left[\sqrt{1 - \left(\frac{p}{R}\right)^2 \sin^2 \phi} + \left(\frac{p}{R}\right) \cos \phi \right] \quad (5)$$

The total amount of photons is therefore:

$$N = 2\alpha I \sin(2\theta) R \int_0^{\phi^*} \sqrt{1 - \left(\frac{p}{R}\right)^2 \sin^2 \phi} d\phi \quad (6)$$

with

$$\phi^* = \begin{cases} \phi_{max} & \text{for } p > R \\ \frac{\pi}{2} & \text{for } p \leq R \end{cases}$$

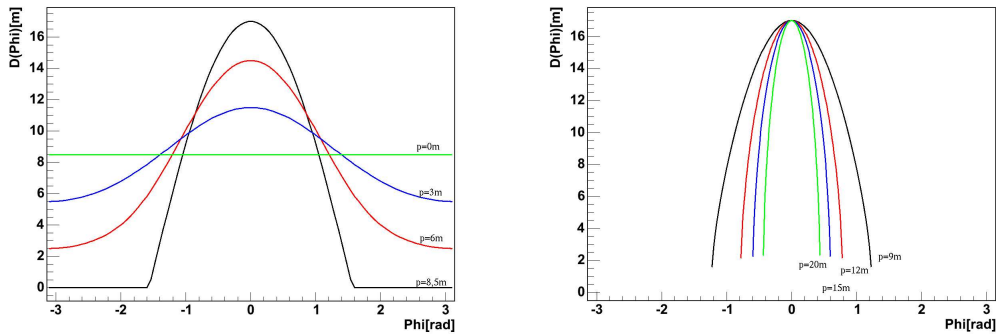


Figure 3: Intensity distribution along the ring for different impact parameter from eqn. 4 and eqn. 5 (Radius of the mirror $R = 8.5$ m), on the left panel for muon impact inside and on the right panel for outside the mirror dish.

Figure 4 shows a muon ring, recorded with the MAGIC camera and its azimuthal intensity distribution (fHistPhi).

2.2 Broadening of the muon ring image

Different reasons lead to a broadening of the muon ring image. They can be distinguished in physical and technical reasons [3]. The physical reasons mean, that the muon ring image has an intrinsic broadening, because the Čerenkov radiation from the single muon is not exactly parallel. These reasons are the following:

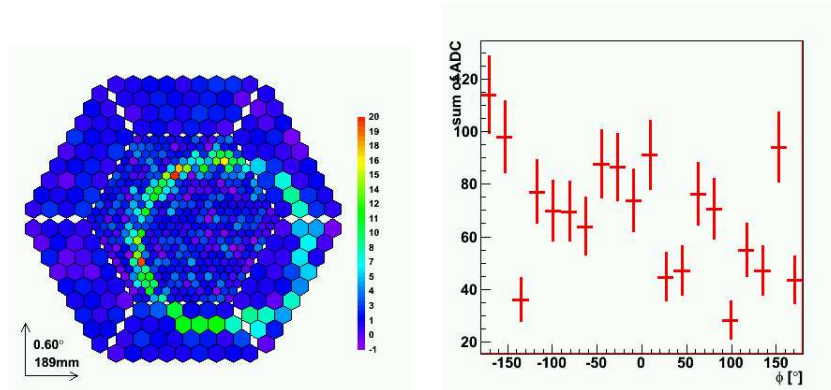


Figure 4: Muonen image in the MAGIC camera. The left panel shows a full circle, the right panel its azimuthal intensity distribution (fHistPhi)

1. Changes in the refractive index: Refractive index in atmosphere is depending on altitude and wave length. The relative broadening decreases with increasing muon energy. It reaches a minimal value of about 1%.
2. Multiple scattering: Due to Coulomb scattering, which affect the muon along its path, the Čerenkov photons are scattered around their expected position in the focal plane. Their distribution is approximatly gaussian. The relative broadening due to this effect is about 8% at a muon energy of 10 GeV. With increasing energy it is rapidly decreasing.
3. Ionisation loses: Due to ionisation, muons lose energy on their way through atmosphere, which results in a smaller Čerenkov angle. This causes a broadening of less than 1%.

Other reasons for the broadening are technical ones:

1. Pixel size: The uncertenty of the determination of the radius, due to discretisation of the image in the camera is dependend on the amount of pixels, that are used for the calculation. Due to the small inner pixels of the MAGIC camera, the broadening for a full ring is just 0,5%.
2. Aberration: The reflector of MAGIC is parabolic, but with spherical mirror panels. The spherical aberration of the small sinlge mirrors is superposed by the much higher coma aberration.
3. Misalignment: Due to the bending of the telescope structure, refocussing by an active mirror control (amc) is necessary. If the amc does not work properly, a significant degradation of the psf is visible.

Figure 5 shows the relative broadening vs. muon energy for all effects, despite of the misalignment. For the aberration, an average value of $0,05^\circ$ for the sigma value of a gaussian fit was assumed.

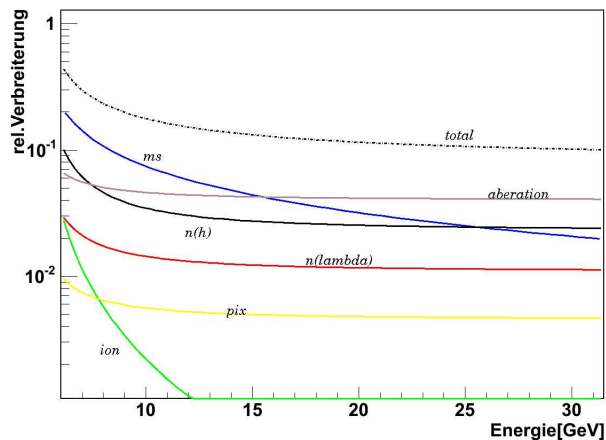


Figure 5: Relative broadening vs muon energy.

3 Method

For the description of muon ring images, some new image parameters are introduced. These are the radius of the ring (Radius), the width of the ring (ArcWidth), the total intensity of the muon image (MuonSize) and the opening angle of the ring fraction (ArcPhi).

3.1 Calculation of the image parameters

The search for muon ring images starts after image cleaning. For this study an absolute image cleaning was applied with 8.5 photo-electrons for core and 4 photo-electrons for boundary pixels.

Every image is fitted by a circle, radius, center of the circle and deviation are calculated. The algorithm starts at the center of the Hillas ellipse (Hillas parameter are calculated before). From that start point the distance to every pixel is calculated and from these the mean value (weighted by the pixel content) with its deviation. The algorithm minimizes the deviation by changing the coordinates of the assumed center. This calculation is made in `MMuonSearchParCalc`, the results are saved in `MMuonSearchPar`. For the minimization, `TMinuit` with the "simplex" algorithm is used. In the second step the event before image cleaning is used and two histograms are filled. One with the radial (`fHistWidth`) and one with the azimuthal (`fHistPhi`) intensity distribution. This is made by `MHSinglemuon`. Use:

```
MHFill fillmuon("MHSingleMuon", "", "FillMuon");
tlist.AddToList(&fillmuon);
```

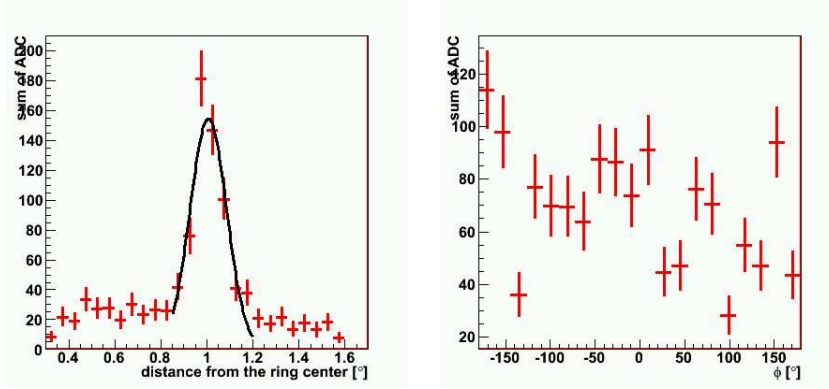


Figure 6: Radial intensity distribution with a gaussian fit (left). Azimuthal intensity distribution (right).

For the radial intensity distribution, only inner pixels are used. For the azimuthal intensity distribution, all pixels inside a certain margin (default: 0.2°) around the radius are used. In both histograms, the same algorithm is searching for the signal region. Only the part of the histogram, which bin content is over a certain threshold (default: 30 phe) is supposed to belong to the signal. ArcWidth is defined as the sigma value of a gaussian fit to the signal region in fHistWidth. ArcPhi is just the sum of connected bins, which are over the threshold. These calculations are made by MMuonCalibParCalc. The parameters are saved in MMuonCalibPar. The thresholds as well as the margin are saved in a separated class, called MMuonSetup. Read also the class documentation for more details. MuonSize is defined as sum of the contents of all pixels along the ring inside the margin, independent of the calculated ArcPhi.

To distinguish between muon and non-muon events, it is necessary to introduce cuts in the new parameter space. Some of these cuts can be made between two steps of calculation to save computing time. A cut in Hillas-Size of 150 phe is recommended as a precut. After calculation of Radius, a cut in Radius and deviation can be made. For this study the following cut were made:

- $180 \text{ mm} < \text{Radius} < 400 \text{ mm}$ (0.61° and 1.35°)
- $\text{deviation} < 35 \text{ mm}$ (0.12°)
- $0.04^\circ < \text{ArcWidth} < 0.20^\circ$
- $\text{ArcPhi} \geq 198^\circ$

The cut in ArcPhi is very powerful and corresponds to the condition, that the muon hit the reflector.

3.2 Simulation

About 65000 muons were simulated with the Magic Monte Carlo Simulation (MMCS) program, which is based on the simulation program CORSIKA from KASCADE group (version 5.20) [4]. Starting altitude was ~ 1 km above observation level, distributed randomly in a cone 1.5° around the vertical axis. The telescope was pointing to the zenith, impact parameter was randomly distributed from 0 m to 12 m. The spectra, which is taken from [1], is simulated from 6 GeV to 80 GeV in three subsamples with different slopes.

- (6-10) GeV, 34000 muons with $dN/dE \sim E^{-2,16}$
- (10-20) GeV, 21750 muons with $dN/dE \sim E^{-2,46}$
- (20-80) GeV, 9520 muons with $dN/dE \sim E^{-2,71}$

3.3 Results

For the following comparison, a data sample from september the 22nd, where the Crab Nebula was observed, is used (sequence 39289). The observation time is 114 min with zenith distance from 14° to 45° .

Simulation and observational data show acceptable agreement in all basic muon parameters.

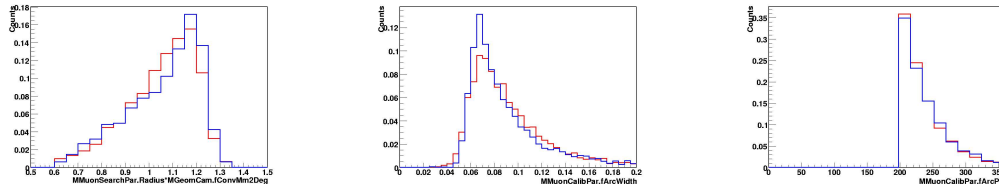


Figure 7: Distribution of basic muon parameters Radius(left), ArcWidth (middle) and ArcPhi (right) for observational data (red) and simulated data (blue).

3.4 Point-Spread function and overall light efficiency

As the muon ring has an intrinsic broadening, the absolute value of ArcWidth is not equal to the sigma value for the psf. To get the size of the psf it is necessary to compare simulated muons with different psf with muons extracted from observational data. To get the relative ring broadening vs. energy, ArcWidth divided by Radius vs. Radius is plotted in a TProfile histogram for simulated and observational data. To get a value for describing the agreement, the ratio of

both histograms is also plotted and the average ratio is calculated (fig.8). In this distribution, the first bins and the last bins show disagreement. These are border effect, due to over- or underestimation of the correct ring radius. Exspecially for small radii, the effects of broadening from the atmosphere is much higher and maybe worse simulated. For further analysis, these bins are excluded. As shown in section2 the total intensity of the muon ring image is

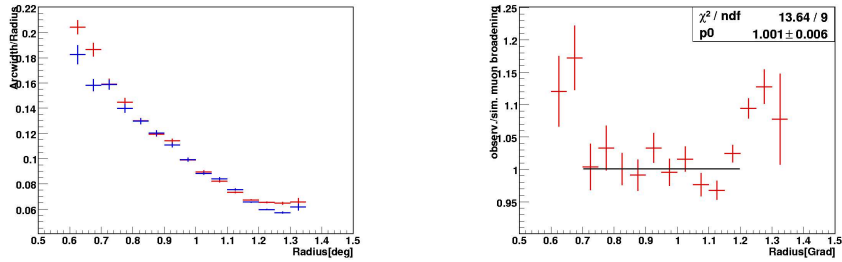


Figure 8: Left panel: ArcWidth/Radius vs Radius for the test sample (red) and simulated muons (blue) with a psf of 12.2mm (10 mm additional spot size). Right panel: The ratio of both distributions, fitted by a constant.

nearly linear in the radius. To measure the overall efficiency and to be sure, that simulated data fit the observational data, MuonSize vs Radius is plotted for both in a TProfile plot. The ratio of both histograms is also plotted and the average ratio is calculated (fig.9). Like for the broadening, only the bins from Radius 0.7° to 1.2° are taken for the analysis.

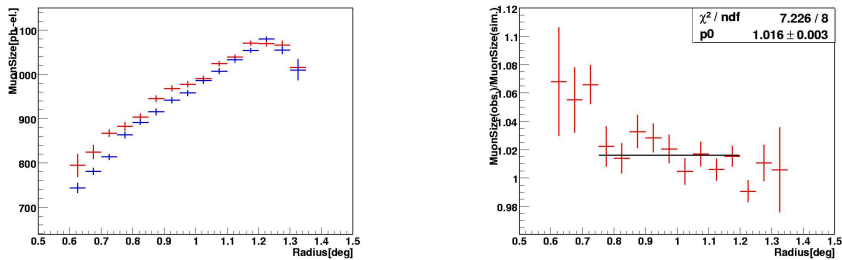


Figure 9: Left panel: MuonSize vs Radius for the test sample (red) and simulated muons (blue). Right panel: The ratio of both distributions, fitted by a constant.

4 Automatisation

As muon ring images were recorded with a rate of ~ 1 Hz, the psf and the light efficiency can be calculated every 10 min to 20 min. That means, that even for most of the smaller sequences, a reliable analysis with enough statistic is possible.

4.1 Implementation in the standard analysis chain

Due to the huge amount of data, it is important to automatisize as much as possible of analysis. Also the muon ring analysis is implemented now in the standard analysis chain, namely in `star`, where the other image parameters are calculated so far.

A new class, called `MHMuonPar`, displays the most important muon parameters (Radius, ArcWidth, Size vs. Radius, ArcWidth/Radius vs. Radius) in a `MStatusDisplay`.

The plots are filled only for events, which survive the cuts, described in section 3. The default values as well as the setup values for the analysis, can be changed in the `star` configuration file (`star.rc`).

All muon parameters are only calculated for muon-like events, to save computing time and to reduce the output. The muon parameters are stored in a separate tree, called "Muons". In this tree, there are also stored all other parameters again for these events.

4.2 Simplification of the psf and light collection efficiency calculation

As both informations can only be calculated by comparing the observational data with simulation, it is necessary to plot both for further investigation. If the shape of the distributions is the same, it is enough to compare just the integral values both from the Size vs. Radius and from the relative broadening plot. For the default parameter settings these integrals were calculated for simulated muons with different psf. Figure 10 shows the results. By calculating the same integral for the muon rings of the observational data, one gets the psf (sigma of a gaussian distribution in mm) as:

$$\sigma_{\text{psf}} = \frac{\text{int}_{\text{psf}} - 0.736}{0.0276} \quad (7)$$

For the determination of the ratio `MuonSize` of observational data to `MuonSize` of simulated data, one has to take into account, the dependence of the `MuonSize` integral on the psf (fig. 10, right plot). One gets the ratio as:

$$\text{ratio} = \frac{\text{int}_{\text{size}}}{9750 - 26.1 \sigma_{\text{psf}}} \quad (8)$$

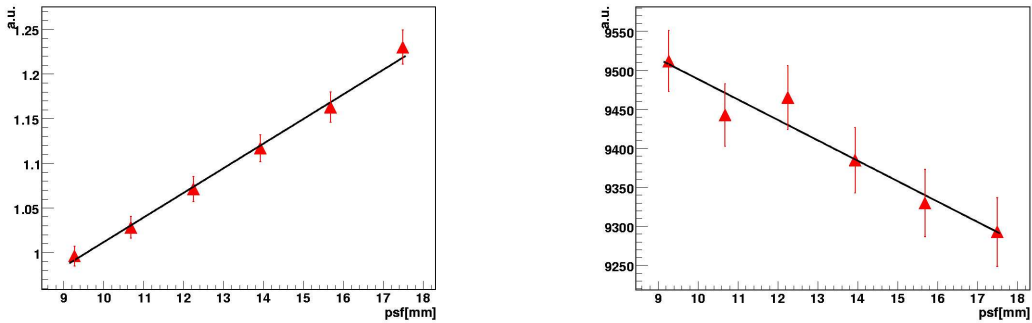


Figure 10: Integral of ArcWidth/Radius vs psf (left plot). Integral of MuonSize vs psf (right plot).

The psf and the intensity of observational muons in the ratio of simulated ones are available in the database and can be plotted with the macro "plodb.C", even for single periods or single nights.

The reference values, calculated from the simulated muon data, depend on calibration, image cleaning, threshold settings in the muon analysis and the cuts, which are applied for the selection of the muon events.

5 Stability and performance study

In this section, the muon parameters for all MAGIC data from june 2004 to april 2005, which could be calibrated automatically in the data base, are shown. First it's important to know how reliable the muon analysis is. After that the performance of telescope for the last ten month is discussed. Due to the statistic, needed for the muon analysis, 400 muon events or more are recommended. Appendix A shows the distribution of psf, ratio and muon rate after a cut in the number of muons. Most of the outliers are disappeared after the cut.

5.1 Muon rate

From BESS measurements, one would expect a rate of about 4 Hz, assuming an effective FOV of $\sim 1^\circ$ and an area of $\sim 230 \text{ m}^2$. The measured rate for low zenith distances is $\sim 1.1 \text{ Hz}$ and decreases for higher zenith distances. The lower rate dependence on the selection criteria and can be understood as a single muon rate, because muons are often accompanied by electromagnetic sub-showers. The rate shows also a weak dependence on the psf. Also a loss of muon events due to the hard tail cuts is expected.

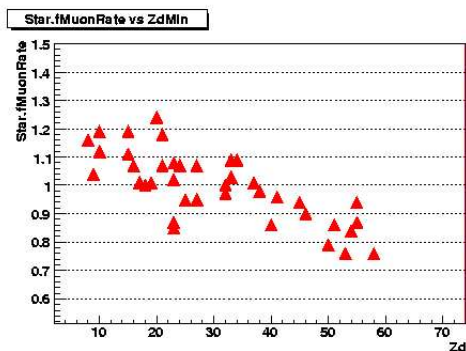


Figure 11: Muon rate versus zenith distance for period 21.

5.2 Point-spread function

The distribution of the psf versus time shows that the psf of the reflector of the MAGIC telescope has first improved after the new mirror alignment in july by $\sim 40\%$.

In the late summer and autumn of 2004 the psf was increasing slowly and after a bad-weather period in february (period 26), the psf was much worse than before the mirror alignment in 2004. Looking more into the details, the calculated psf

Table 1: Psf [mm] for the last eleven observation periods. The number is the mean value from a gaussian fit to the psf distribution and the sigma value. In period 19 and 26 no data were taken. The data of period 27 could not be calibrated by the standard analysis due to problems with the pulse position. 400 muons and more are required for every sequence, which is taken into account.

period	psf[mm]
18	16.7 ± 1.5
20	11.0 ± 1.3
21	11.2 ± 1.7
22	12.8 ± 1.4
23	13.8 ± 1.0
24	14.3 ± 1.8
25	13.7 ± 1.0
28	16.7 ± 0.7

has a spread of more than two millimeters, even for single nights. Some outliers could be identified as moon data. Due to fact, that the simulation was done

without the influence of the moon, these values are not reliable. Up to now, no correlation to other parameters could be found, neither the zenith distance nor the number of errors of laser adjustment.

While the statistic error of the psf calculation for a single sequence is less than 1 mm, the systematic error seems to be by a factor two higher. The total error is estimated to be about 2 mm.

5.3 Calibration

The distribution of the intensity ratio over time shows difference between data, where the signal is extracted with the DigitalFilter-method and data, where this is done with the Spline method. The "Spline" was mostly used for this data from november the 17th in 2004 to the end of january 2005, but also for some single sequences in september and october 2004.

For the simulated data in this study, only the DigitalFilter-method with the "Monte Carlo weights-file" was used for the signal extraction. For the simulated calibration runs, the calibration weights-file, which is also used for the "real" calibration runs was used. The simulation output is reduced by 27 %, due to the first results of muon analysis, made by Keiichi Mase in october 2004.

After analysis of the september and october data an average intensity of observational muons in the ratio of simulated ones of 1.04 was found (Digital Filter) while for december data (Spline) the ratio was 1.11. To get all observational data at the same intensity level, all data were calibrated again, whereas the conversion factors are divided by a correction value (1.04 and 1.11 for digital filter and spline respective). Table 2 shows the mean ratio with standard deviation for each period, after a gaussian fit to the ratio distribution. The plots are in appendix B.

The spread, even for single nights, is less than 3 %.

6 Summary

Muon ring images can be easily reconstructed and separated from other images. Due to their well defined azimuthal and radial intensity distribution, they can be used to calculate the point-spread function (psf) as well as the total light collection efficiency.

For the analysis of muon ring images, a set of new image parameters are introduced. These are the radius of the ring (Radius), the width of the ring (ArcWidth), its length as a fraction of a full ring (ArcPhi) and its total light content, measured in photoelectrons (MuonSize). The agreement to muon events from Monte Carlo simulations is acceptable.

For the calculation of the psf, the relative broadening of the ring (ArcWidth di-

Table 2: Ratio [%] for the last eleven observation periods. The number is the mean value with its standard deviation to a gaussian fit to the ratio distribution. For period 24 the mean value and the rms of the histogram is used because of the statistic was too less for a fit. In period 19 and 26 no data were taken. The data of period 27 could not be calibrated by the standard analysis due to problems with the pulse position. 400 muons and more are required for every sequence, which is taken into account.

period	ratio[%]
18	104.1±1.5
20	102.9±1.8
21	101.2±1.3
22	101.9±2.2
23	101.9±2.2
24	100.7±2.7
25	99.5±1.7
28	97.6±1.6

vided by Radius versus Radius) is used. Due to the intrinsic broadening, it is necessary to compare the broadening from muon extracted from observational data to simulated muons with different psf. To simplify this method, just the integral value from the relative broadening plot is compared to reference value from simulated muons, calculated before, after the same selection criteria.

For the determination of the light collection efficiency, the intensity (MuonSize versus Radius) of observational muons is compared to that of simulated ones. the method can be simplified in the same way like for the psf calculation, whereas the correct psf has taken into account.

The muon analysis is now full implemented in the standard analysis chain. The calculation of muon parameters is made by star, changes of the selection criteria or the analysis parameters can be done in the configuration file of star (star.rc). The image parameters of muon events are written in a separated tree (Muons). The psf as well as the ratio between the intensity of observational and simulated data is now available in the database. To ensure reliable results, a number of more than 400 muon events are recommended. Data, which are taken by moon light are also skipped, because the influence of the moon light to the night sky background was not taken into account in the simulation.

The psf shows an improvement of about 40% after the new mirror alignment in july 2004. In the late summer and autumn the psf was getting worse. After a bad weather period in february 2005, the psf has increased again. the the psf, even for a single night is about two millimeters and shows no correlations to other paramters.

around 100% for summer and autumn DigitalFilter-method. The december and

extracted with the Spline-method, the ratio is spring the ratio is again smaller and decreases be understood from the degradation of the single nights is smaller than 3%. The intensity ratio is stable around 100% for nearly all data after dividing the conversion factors by a correction value (1.04 for digital filter and 1.11 for spline data respectively) as calculated before with the muon analysis. could be understood from the degradation of the for single nights is smaller than 4%.

References

- [1] M. Motoki et al., 2003, *Astroparticle Physics*, 19, 113
- [2] A. C. Rovero et al., 1996, *Astroparticle Physics*, 5, 27
- [3] G. Vacanti et al., 1994, *Astroparticle Physics*, 2, 1
- [4] D.Heck; J.Knapp et al., 1998, FZKA-6019

A Overview

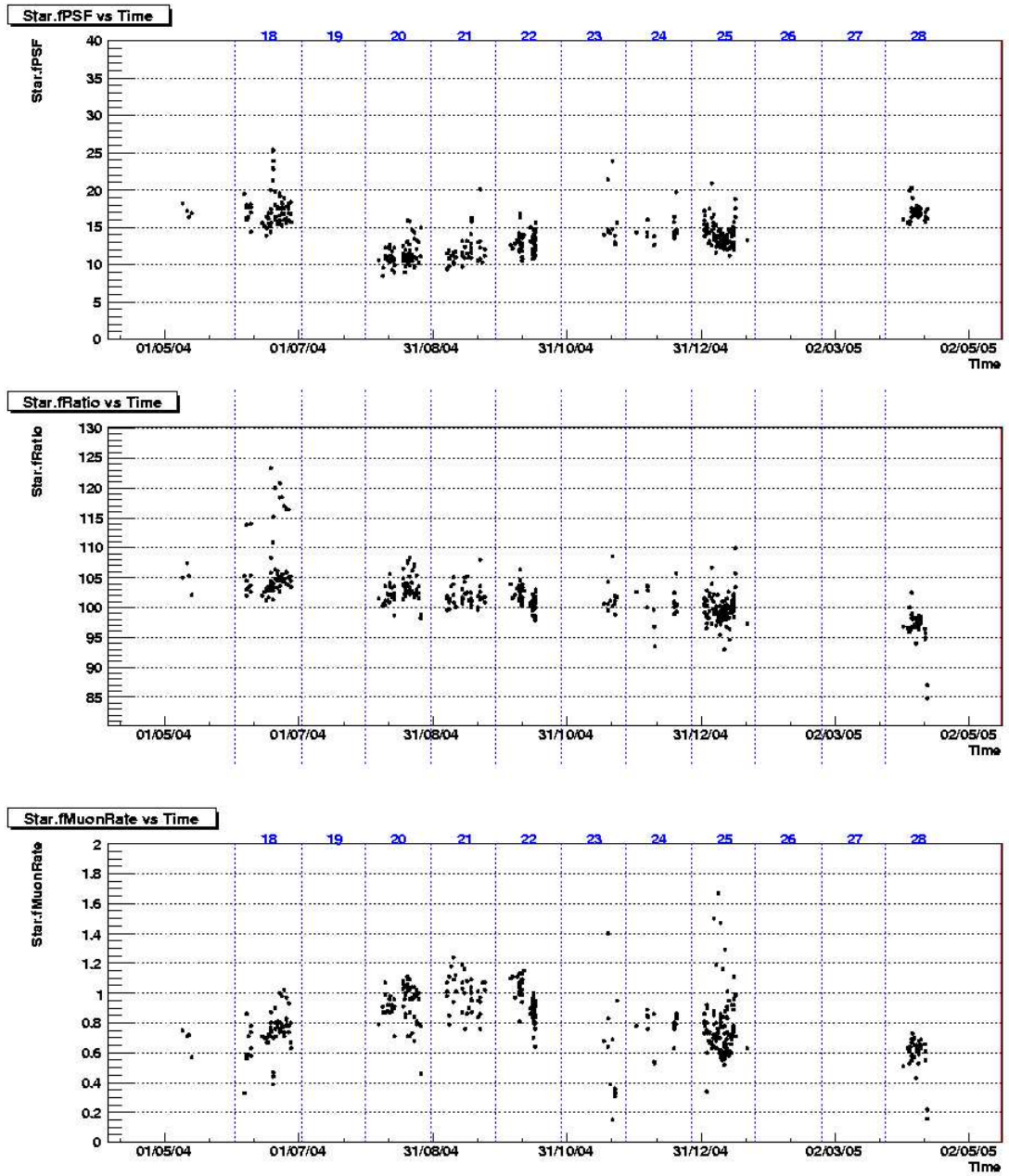


Figure 12: Psf, ratio and muon rate versus time. Every point represent one sequence, which contents more than 400 muons.

B Point-spread function

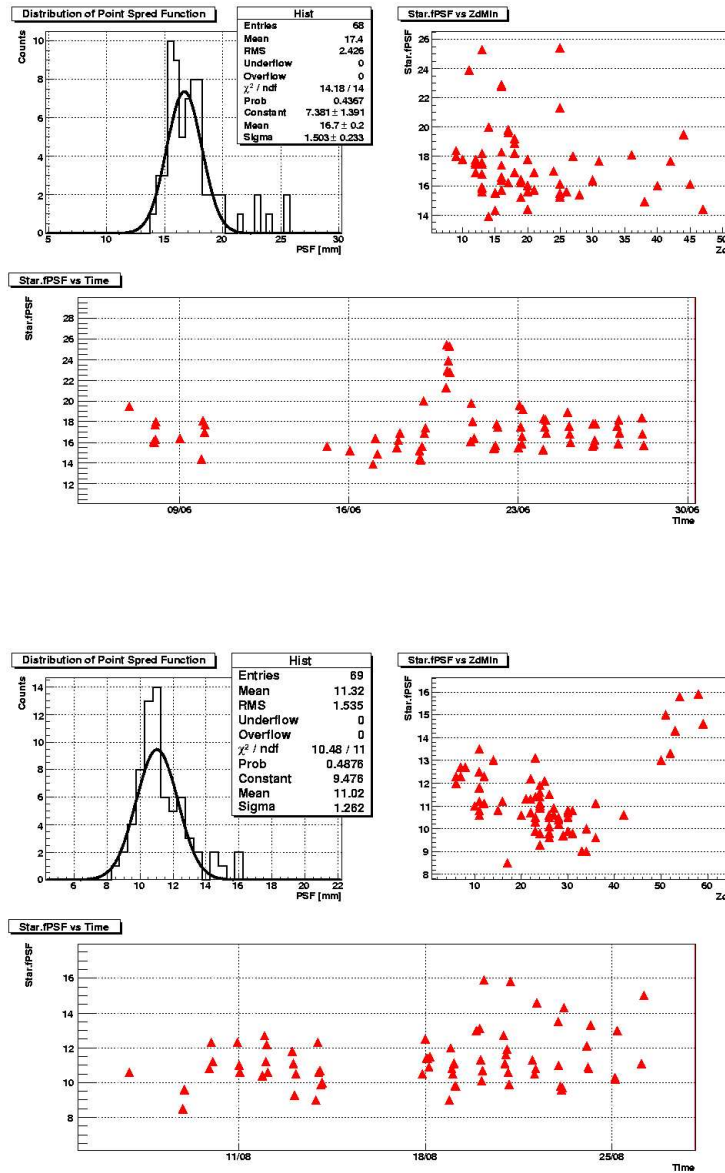


Figure 13: Psf of period 18 (june 2004, upper panel) and period 20 (august 2004, lower panel) with a gaussian fit. Every triangle represent one sequence, which contents more than 400 muons.

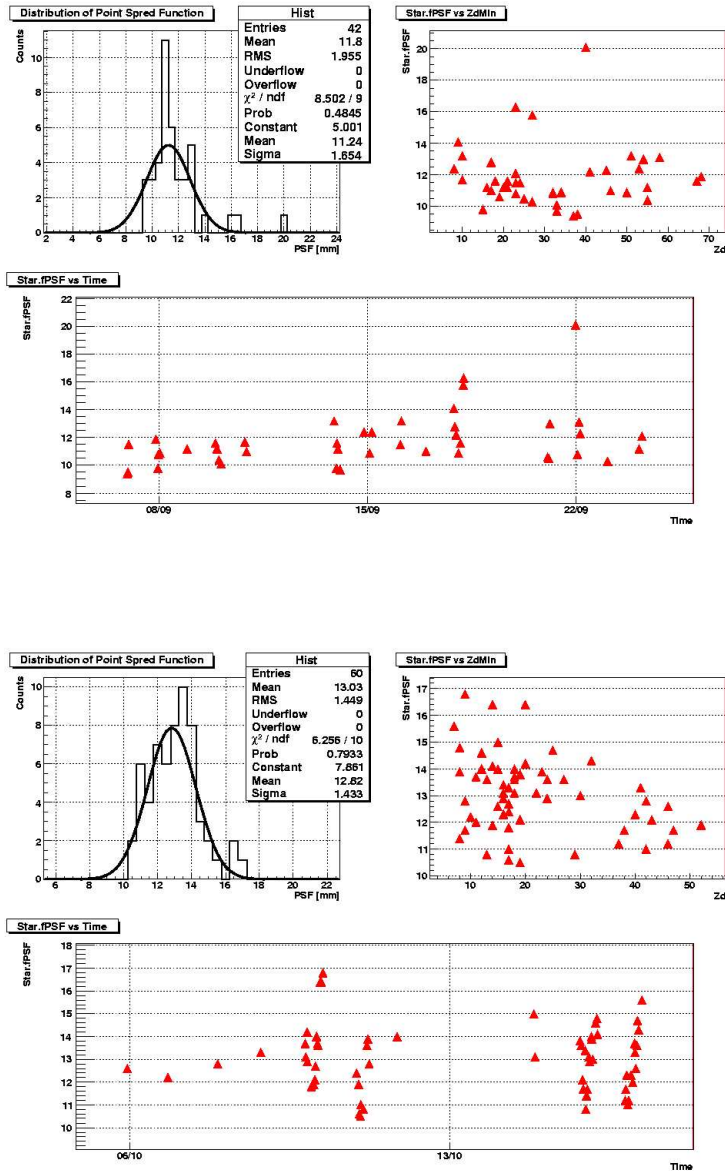


Figure 14: Psf of period 21 (september 2004, upper panel) and period 22 (october 2004, lower panel) with a gaussian fit. Every triangle represent one sequence, which contents more than 400 muons.

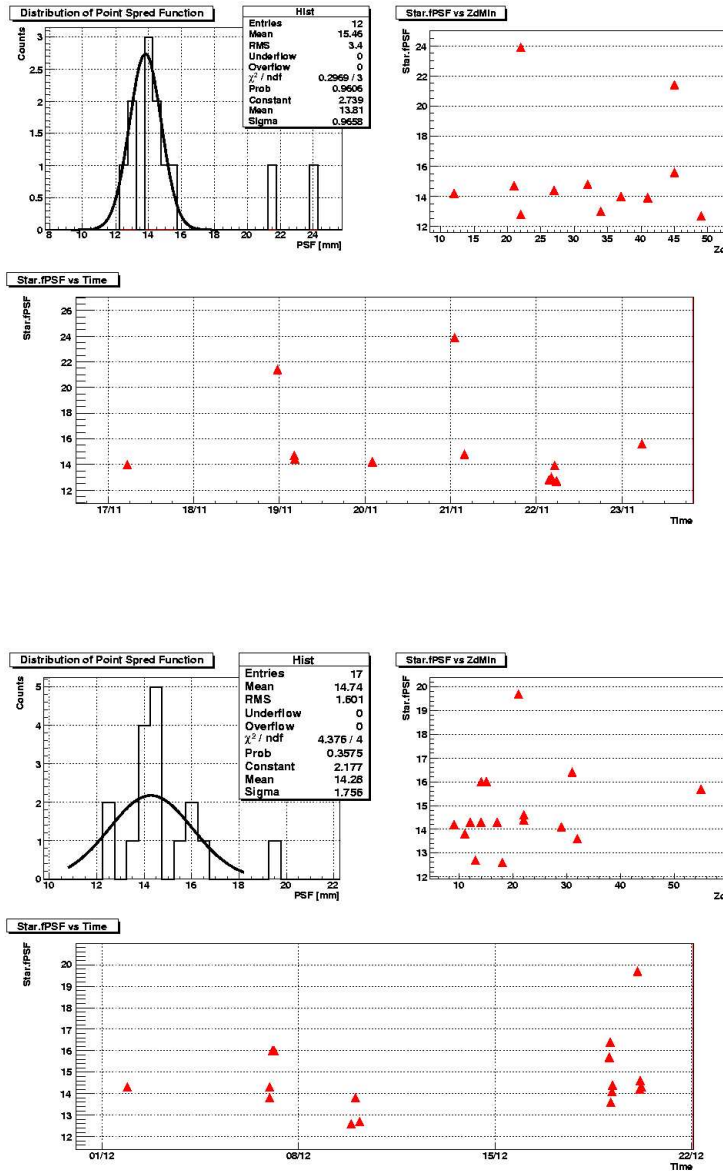


Figure 15: Psf of period 23 (november 2004, upper panel) and period 24 (december 2004, lower panel) with a gaussian fit. The fit quality is poor due to the low statistic in both periods. The outliers in both histograms represent data, taken during moon time. They are therefore not used for the fit. Every triangle represent one sequence, which contents more than 400 muons.

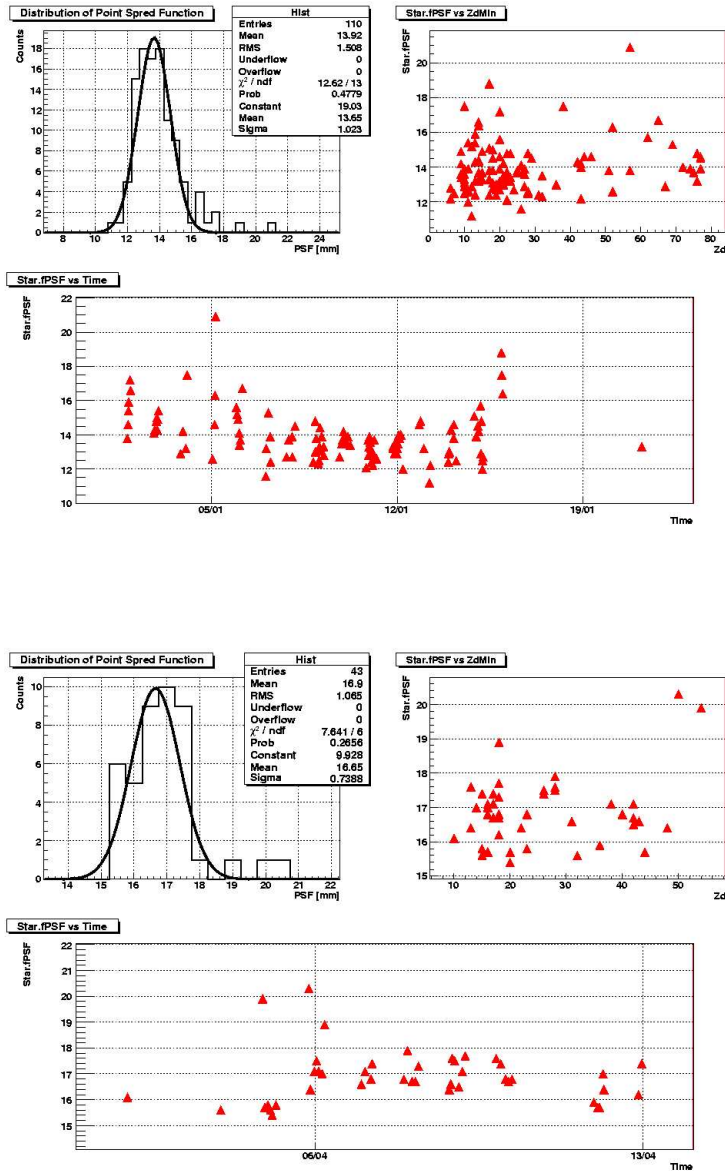


Figure 16: Psf of period 25 (january 2005, upper panel) and period 28 (april 2005, lower panel) with a gaussian fit. Every triangle represent one sequence, which contents more than 400 muons.

C Calibration

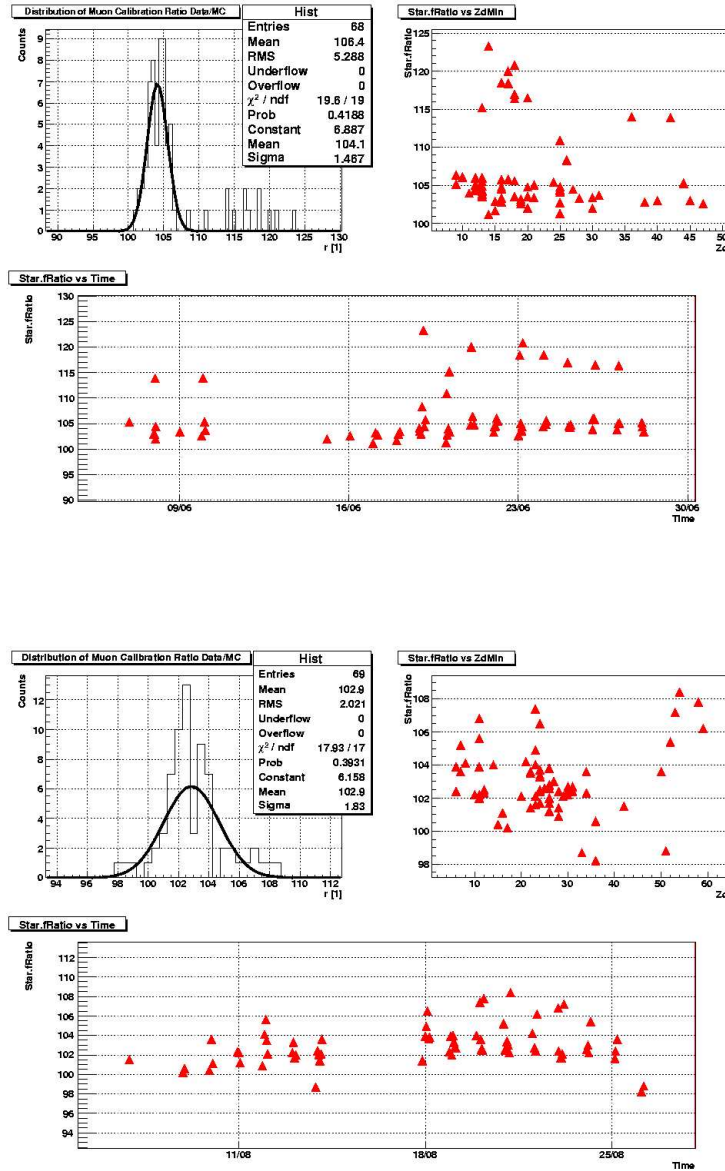


Figure 17: The intensity of observed muons at the ratio of simulated ones for period 18 (june 2004, upper panel) and period 20 (august 2004, lower panel) with a gaussian fit. Every triangle represent one sequence, which contents more than 400 muons.

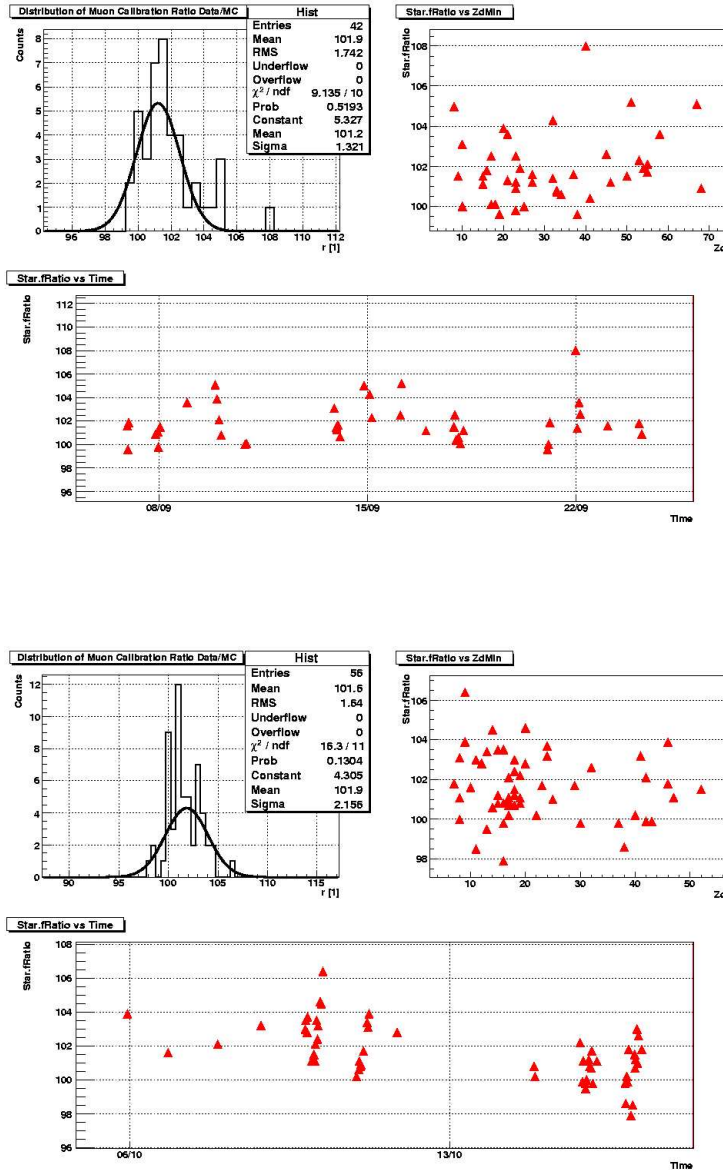


Figure 18: The intensity of observed muons at the ratio of simulated ones for period 21 (september 2004, upper panel) and period 22 (october 2004, lower panel) with a gaussian fit. Every triangle represent one sequence, which contents more than 400 muons.

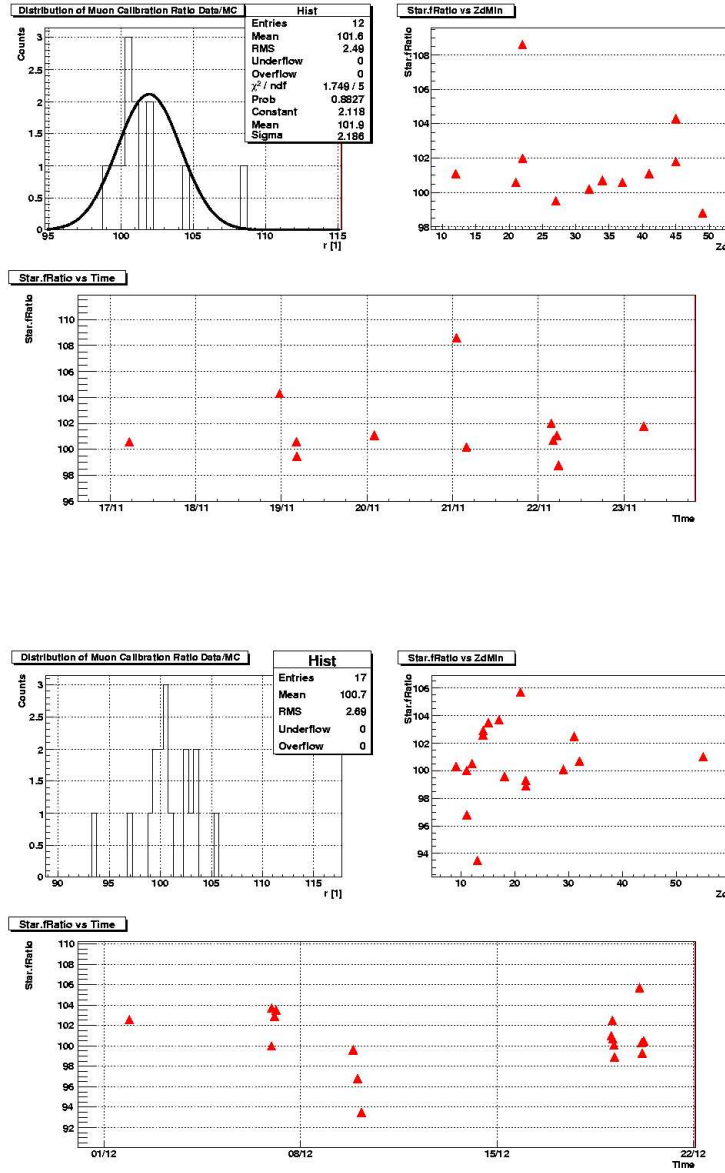


Figure 19: The intensity of observed muons at the ratio of simulated ones for period 23 (november 2004, upper panel) with a gaussian fit and for period 24 (december 2004, lower panel) without the fit due to less statistic. Every triangle represent one sequence, which contents more than 400 muons.

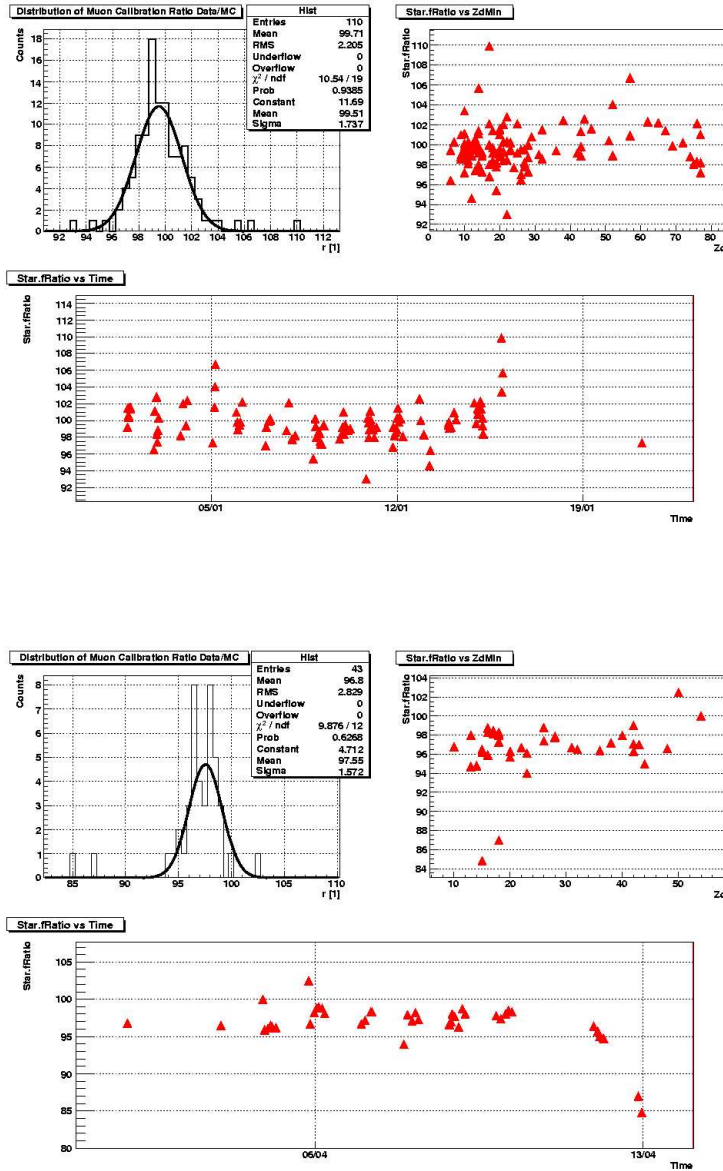


Figure 20: The intensity of observed muons at the ratio of simulated ones for period 25 (January 2005, upper panel) and period 28 (April 2005, lower panel) with a gaussian fit. Every triangle represent one sequence, which contents more than 400 muons.